Mapping the Lithospheric Magnetic Field from CHAMP Scalar and Vector Magnetic Data

Stefan Maus, Kumar Hemant, Martin Rother and Hermann Lühr

GFZ, Div. 2, Telegrafenberg, 14473 Potsdam, *smaus@gfz-potsdam.de*

Summary. Eighteen months into the CHAMP mission there is now a seizable data set of scalar and vector magnetic measurements. With this data the lithospheric magnetic field can be mapped far more accurately than in previous missions.

Key words: geomagnetic field, magnetic anomalies, field models

1 Data Selection

We estimate two separate field models from the CHAMP scalar magnetic data of 9 Aug. 2000 to 30 Sep. 2001, and the vector data of 1 Jun. 2001 to 21-Dec. 2001. From all of the polar latitude data we select a 5% subset of tracks with particularly low residuals. For the lower latitudes, night time data are selected from 22:00 to 6:00 local time (LT), excluding the period of 19:00 to 22:00 LT in order to avoid the sporadic disturbances caused by F region currents [4]. Figure 1 shows the behaviour of mean scalar residuals with the K_p index, which is a three-hour-range index derived from 13 magnetic observatories quantifiyng the effect of solar particle influx on the magnetic field. We use only data at magnetically quiet times, quantified by $K_p \leq 2$.

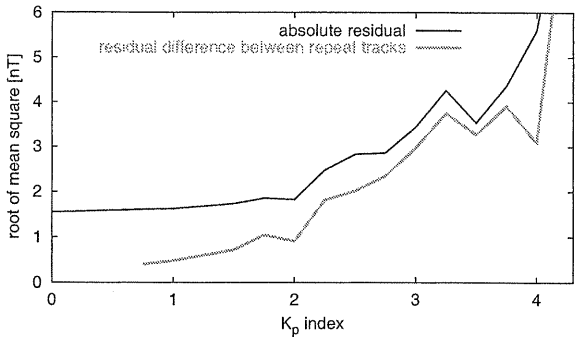

Fig. 1. Along track residual rms for night time low-latitude scalar data against the K_p index. We use only data with $K_p \leq 2$. The residual difference between repeat tracks can be extrapolated to around 0.1 nT for $K_p = 0$, indicating the extraordinary precision of the measurements. In contrast, the corresponding curves for the vector components (not shown here) tend to 1 nT for $K_p = 0$, due to star camera noise.

2 Correction for magnetospheric fields

After the standard main and external field corrections the magnetospheric signal remaining in the data is still of the order of the strength of the lithospheric field (Figure 2a). This is a key issue in lithospheric field mapping. The significant disagreement between earlier lithospheric field models is partly a consequence of using data which still contain significant external field signal. We remove this contribution by fitting and subtracting track by track an external field with the corresponding induced internal fields coupled by Langel's empirical factor of 0.27 to the external fields. This is done to degree-1 for the scalar and to degree-2 for the vector data. Subsequently, the corrected signal is clearly dominated by the lithospheric field (Figure 2b).

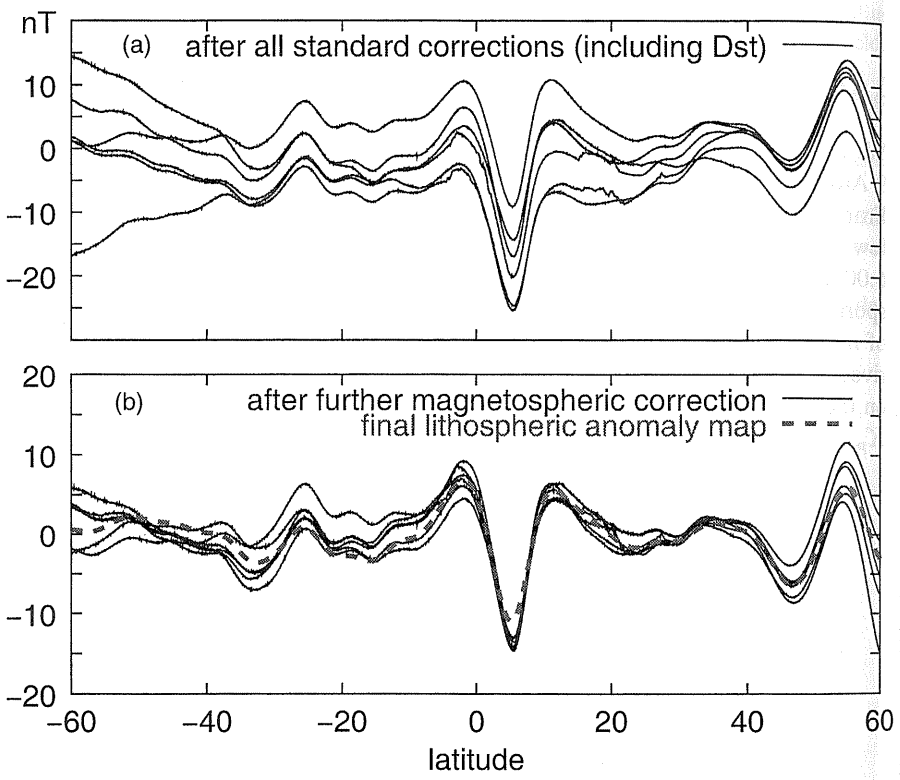

Fig. 2. Night time sample tracks at 20.0°-20.7° longitude. After all standard corrections the remaining residuals (a) are still dominated by external fields. In order to retain as much along-track signal as possible, we only subtract a best fitting homogeneous field from each track (b). Note the signature of the well known Bangui anomaly at 5°N. Underestimation of this peak by our final model (dashed) is due to truncation at spherical harmonic degree 65.

3 Discarding noisy tracks

After the previous corrections, some noisy tracks remain. They can be identified and eliminated by plotting the along-track residual rms against the longitude at the equator crossing (Figure 3).

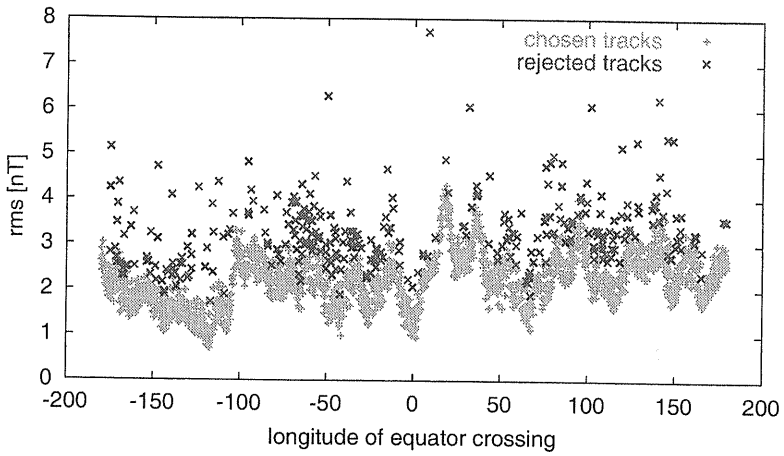

Fig. 3. Noisy tracks are identified and removed using a 4° sliding window in longitudes

4 Field model estimation

A field model is conveniently represented by the coefficients of the spherical harmonic expansion of the scalar magnetic potential. These coefficients can be estimated by a least squares inversion. We estimate separate models from the scalar and the vector data in order to get an idea of the uncertainties involved. Later, a joint model will be generated. In the case of scalar-only data, a minimum norm solution is sought, due to the ambiguity caused by the Backus effect.

5 Comparison with other field models

Apart from visual comparisons, which are given in a companion paper in this volume, there are statistical tools for gaining insight into the differences between models. The first is the spherical harmonic power spectrum (Figure 4). The strong differences in power between field models reflect the ambiguity between magnetospheric and ionospheric contamination on the one side and along-track trending lithospheric anomalies on the other. The models with higher power rely on carefully selected but

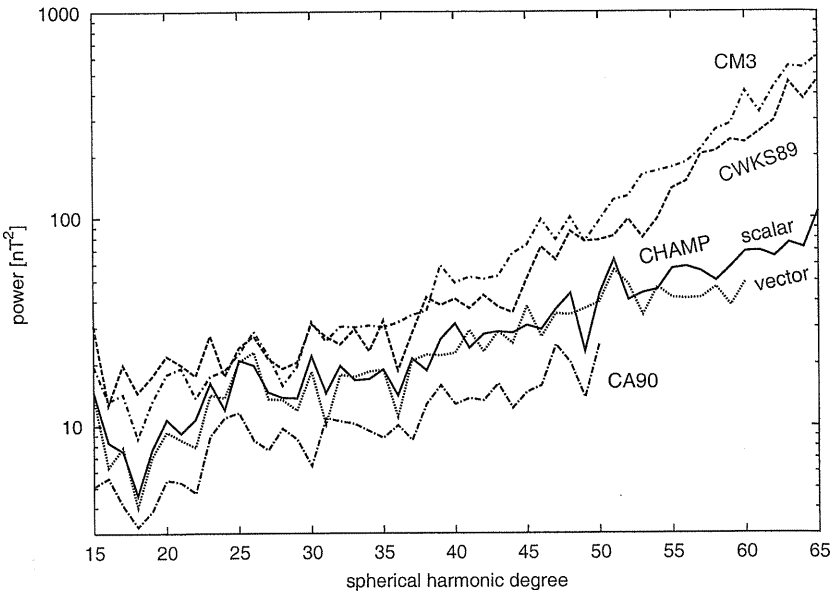

Fig. 4. Magnetic power spectra of CA90 [3], CWKS89 [2], CM3 [7], and our CHAMP scalar and vector field models. The main reason for the upward slope in the power spectra is the peculiar definition of the Mauersberger/Lowes spectrum, which slopes upward for a spatially uncorrelated magnetic field [6]

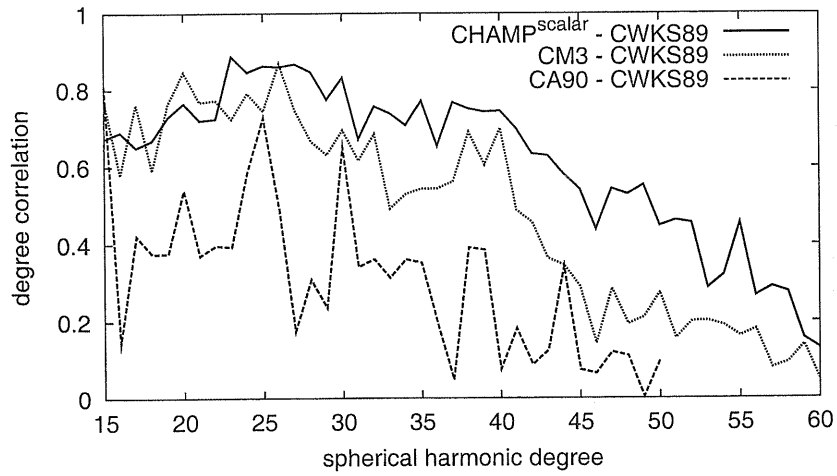

Fig. 5. Correlations of model CWKS89 with models CM3, CA90 and our scalar field model.

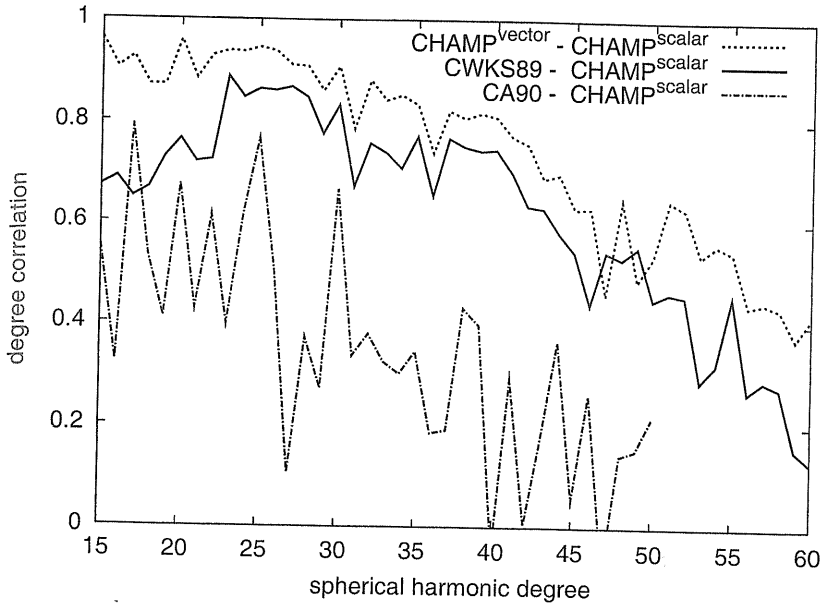

Fig. 6. Correlations of our scalar field model with CWKS89, CA90 and our vector field model.

unfiltered data, while the lower power models rely on various techniques of track-by-track external field removal. The true strength of the lithospheric field must lie somewhere in between.

Further insight is provided by the average correlation between the coefficients of two models, separately for each degree [1]. Two sets of degree correlation curves are shown in Figures 5 and 6. As may have been expected from the power spectra, the correlation between different models is rather poor. Interestingly, our model from scalar-only CHAMP data has the highest correlation with CWKS, despite the uncertainty known as Backus' effect (Figure 5). The higher correlation among the CHAMP scalar and vector models (Figure 6) is partly a consequence of using a similar processing scheme for both kinds of data. But it also shows that significant gains in accuracy are possible with the new CHAMP data.

6 A map of B_z at 450 km altitude

Since the scalar-only model has already been published elsewhere [5], we show our preliminary vector-only model in Figure 7.

Acknowledgement. This study was carried out under the grant of the German Federal Ministry of Education and Research (BMBF) No. 03F0333a.

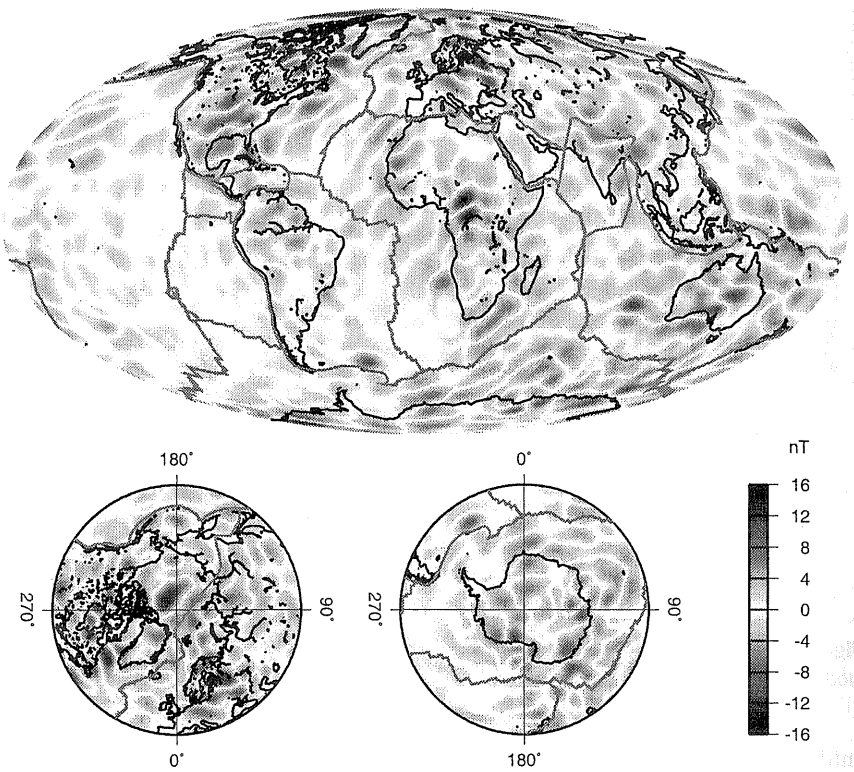

Fig. 7. Downward (B_z) component at 450 km altitude of our preliminary lithospheric field model derived from vector data only.

References

1. Arkani-Hamed J, Langel RA, and Purucker M (1994) Scalar magnetic anomaly maps of Earth derived from POGO and Magsat data, *J Geophys Res*, *99*, 24,075–24,090.
2. Cain JC, Wang Z, Kluth C and Schmitz DR (1989) Derivation of a geomagnetic model to n = 63, *Geophys J Int*, *97*, 431–441
3. Cohen Y, and Achache J (1990) New global vector magnetic anomaly maps derived from Magsat data, *J Geophys Res*, *95*, 10,783–10,800.
4. Lühr H, Maus S, Rother M and Cooke D (2002) First in situ observation of night time F region currents with the champ satellite, *Geoph Res Lett, in print*.
5. Maus S, Rother M, Holme R, Lühr H, Olsen N, and Haak V (2002) First scalar magnetic anomaly map from CHAMP satellite data indicates weak lithospheric field, *Geoph Res Lett, in print*.
6. Maus S (2001)*New statistical methods in gravity and magnetics*, Habilitation thesis, University of Braunschweig, http://www.gwdg.de/~smaus/habil.pdf.
7. Sabaka TJ, Olsen N, and Langel RA (2000) A comprehensive model of the near-Earth magnetic field: phase 3, *Technical Report, NASA/TM-2000-209894*.